

1.2 MV, 800 kA, 150 ns PULSED POWER GENERATOR FOR POWERING FIELD REVERSED ION RING EXPERIMENTS

*D.E. Anderson and J.B. Greenly
Laboratory of Plasma Studies
Cornell University, Ithaca, NY 14853*

*S.C. Glidden and M. Richter
Applied Pulsed Power, Inc.
140 Langmuir Lab., 95 Brown Rd., Ithaca, NY 14850*

ABSTRACT

The Field-Reversed Ion Ring Experiment (FIREX) program at Cornell University is designed to reach the goal of producing a field-reversed configuration (FRC) with current carried by an ion ring trapped in a magnetic mirror. Production of an ion-ring FRC is expected to have favorable stability and confinement characteristics for magnetically-confined fusion. Past experimental results, theoretical analysis and ion ring injection simulations were used to determine the electrical requirements of the generator. Following a brief description of the FIREX program, the electrical and mechanical design of a 1.2 MV, 800 kA, 150 ns pulsed power source for driving an Exploding Metal Foil active Anode Plasma Source (EMFAPS) type ion diode will be described. SPICE circuit analysis results will also be presented.

INTRODUCTION

The new FIREX accelerator is presently in the construction phase at the Laboratory of Plasma Studies at Cornell University. Due to funding and schedule constraints, components from the recently decommissioned LION accelerator (1.2 MV, 300 kA, 40 ns) are being used wherever possible. The accelerator shall consist of a bipolar Marx generator with 24 3.0 μ F, 100 kV capacitors charging a 50 nF triaxial water dielectric intermediate storage capacitor (ISC). After an ISC charge time of approximately 1.2 μ s, a self break SF₆ gas switch closes, charging two 60 ns long coaxial pulse-forming water lines in series (2.5 and 3.2 ohms, discharged in parallel). The PFL is connected to a 1.4 Ω , 20 ns output line via the six electrode self break main water switch. Between the output line and the vacuum interface is an 8 electrode prepulse water switch. Inside the output line is a 14 Ω , 80 ns (one way) transit time isolator. The 60 nH vacuum interface is connected to a short (30 cm long) 10 Ω vacuum line on which the ion diode is mounted. The vacuum interface also contains a transmission line and shunt capacitor for diverting a small fraction of the pulse energy to drive the anode foil of the EMFAPS ion diode.

FIREX is intended as a major step toward the realization of a field-reversed Ion Ring or Ion Ring/FRC reactor in which a significant fraction of the azimuthal current is carried by large orbit ions that provide MHD stability to a high- β field-reversed configuration. In earlier work, ion rings with self-field less than 10% of the applied magnetic field were generated. The goal of FIREX is to produce a fully field-reversed ring with 1 MeV protons. Achievement of this goal will be followed by study of the dynamics and lifetime of the ring, and a demonstration of magnetic compression of the ring as an efficient way to scale to higher energy and lifetime. The basic experimental approach follows that of our earlier experiments. An annular proton beam is injected through a magnetic cusp, transforming up to 90% of the proton kinetic energy into rotation. The rotating beam is then axially trapped in a magnetic mirror to form the ion ring. Formation of a field-reversed ring requires at least 40 mC of protons. For FIREX, we have used numerical simulations to arrive at the final choice of design parameters for a new beam generator and magnetic system to achieve this goal. The simulations have been carried out by a new 2-1/2 D (axisymmetric code, FIRE, which incorporates particle-in-cell ring ions and background plasma ions, and a background electron fluid, and includes collisions of these species with each other and with background neutrals. The code incorporates temporal profiles of injected ion beam voltage and current, derived from simulations of the electrical design of the pulser

combined with experimental data on beam generation in the same parameter range. The code injects this beam into calculated magnetic fields of coilsets and partially penetrable boundary elements of the experimental system. The simulations are evaluated critically by comparison with analytic theory and with previous experimental experience with weak ion rings. Results of the simulations have shown a number of important features of field-reversed ring formation that have been taken advantage of in the experimental design. The proton beam will be generated by a nominal 1.2 MV, 800 kA, 150 ns pulser coupled to a magnetically-insulated ion diode of a type developed over the last decade at Cornell. The beam will be injected through an axially compact magnetic cusp into a gradual ramped solenoidal magnetic field, which rises from 6 to 9 kG over 2 m axial length.

MARX GENERATOR, INTERMEDIATE STORAGE CAPACITOR AND GAS SWITCH

The Marx Generator design was driven by the desire to use the existing LION Marx generator tank and hardware. Twenty-four 3.0 μF , 100 kV Maxwell capacitors will replace the 32 units in the LION generator. Removal of one of the capacitor columns will allow for reuse of all mounting hardware. The Marx switches, Physics International #508, will be refurbished and used. These switches are rated for 140 kA and 2 coulombs for electrode lifetimes of >1000 shots. In FIREX, they will conduct 158 kA and 0.3 to 1.0 C. It is difficult to predict their performance under these operating conditions, but based on the 15 year operation of LION with very few switch failures and limited number of switches used (12), satisfactory performance should be achieved. To insure the tie rods would not be too highly stressed, the forces during switching were calculated to be 267 pounds on each with a peak stress of ~ 2000 psi.

The ISC is composed of three concentric coaxial cylinders, with the outer- and inner-most cylinders nominally at ground potential. The outside diameter of the outer cylinder was limited by the dimensions of the existing LION water tank (2 m). The diameters of the intermediate and inner cylinders were then determined by limiting the electric field on the intermediate conductor to 75% of the positive breakdown strength of water.

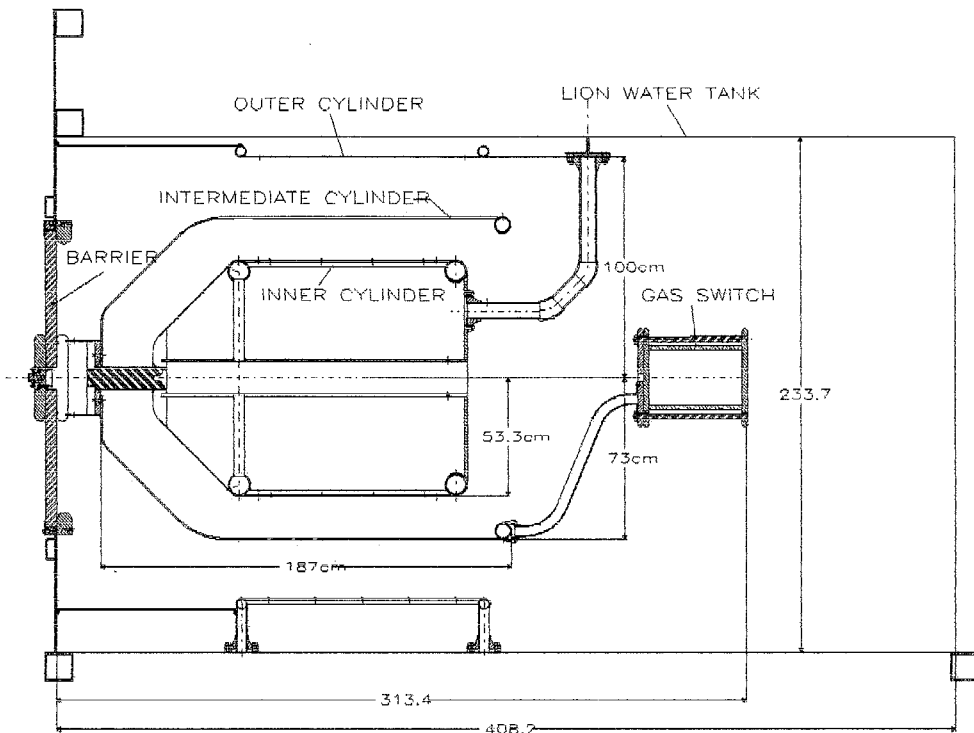


Figure 1 — FIREX ISC Section in Existing LION Tank

Figure 1 shows a sectional view of the ISC. The section shown is through $\phi=90^\circ$ above the centerline and $\phi=240^\circ$ below centerline. In order to keep the electric fields below 100 kV/cm along the surface of the oil-water barrier using the existing LION barrier, it was necessary to ground the inner cylinder at the downstream end of the ISC. The conical shape of the intermediate and inner cylinders was also influenced by this constraint. FEMTO¹, a 2-D electrostatic finite

element code, was used to determine the electric fields and calculate capacitance on the conical section of the ISC.

The ISC intermediate conductor is supported by the oil-water barrier at one end and by three 5 cm diameter tubes connected to the gas switch at the other. The inner conductor is supported at the downstream end by three 7.5 cm diameter tubes and is supported by a 10 cm diameter Delrin rod connected to the intermediate conductor at the other. This Delrin rod support provides inner-to-intermediate conductor alignment in a region where the average electric field is 110 kV/cm, and is easily removable from the downstream end of the ISC in the event surface flashover occurs. The estimated masses of the inner and intermediate conductors are 260 kg, resulting in a maximum stress of 2 MPa (275 psi) on the 2" thick barrier when the conductors are not supported at the downstream end (such as during assembly). This value is well below the ultimate strength (69 MPa) of the cast polyurethane, although the effects of fifteen years' exposure to oil and water and the dynamic forces from the water switches is not accounted for.

The gas switch will conduct a peak current of 440 kA and transfer 125 mC in 420 ns. Use of the LION switch, modified to bring the gas lines out of the upstream end, is planned. This switch operates in self-break mode, and has performed reliably for fifteen years on LION, albeit at lower currents and charge transfers.

PFL AND VACUUM INTERFACE

The PFL/Vacuum Interface section of the FIREX pulser is shown in Figure 2. Again the section is taken through the same axis as in Figure 1. In an effort to decrease the overall diameter of the PFL and increase the length to circumference ratio, as well as operate with relaxed electric field values on the conductors, the 1.4 Ω PFL is split into two parallel lines (2.5 and 3.2 Ω). After the main switch closes, the PFL is charged in series and discharges in parallel when the main water switches close.

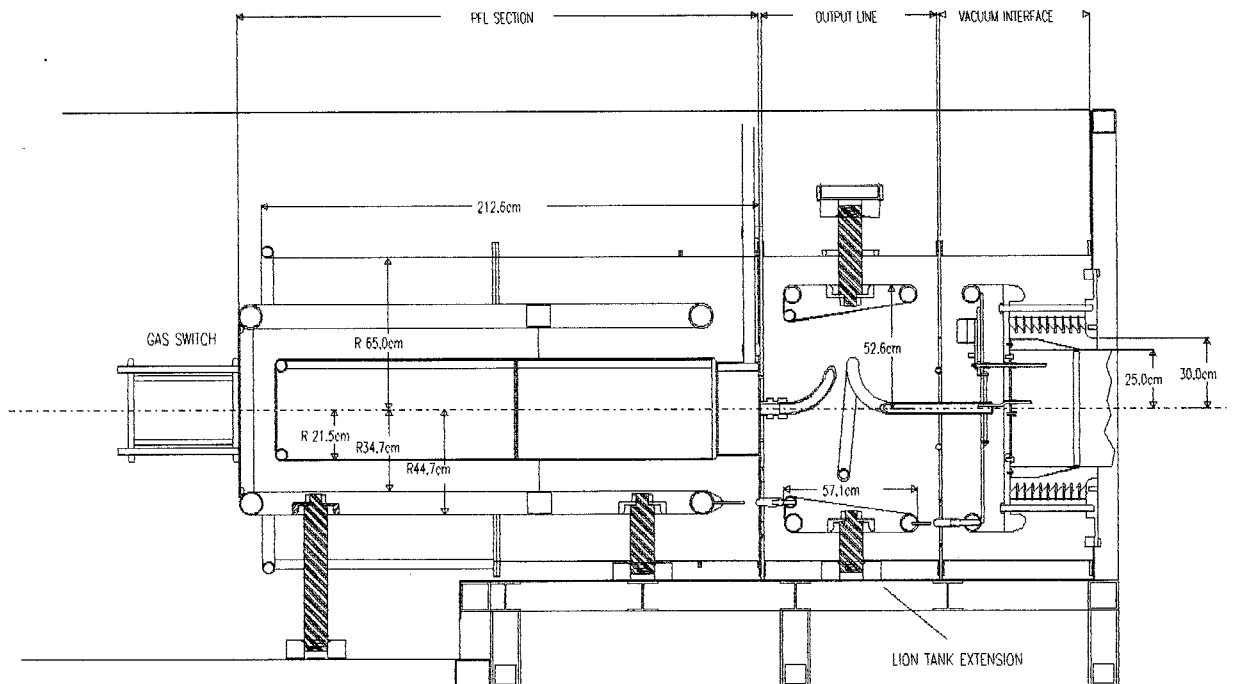


Figure 2 — FIREX PFL/Vacuum Interface Section

The PFL intermediate conductor, with the water switch electrodes, is supported off the base of the tank by four 4" diameter Delrin legs. Grossly oversized clearance holes through the outer conductor and deeply recessed holes in the intermediate conductor increase the surface tracking distance along the legs. The outer conductor is supported at the downstream end by a 3/4" thick aluminum plate and by aluminum legs (not shown) at the upstream end. It is split in two halves, with the upstream half having two longitudinal slots running the length of the part, to facilitate installation. The inner conductor is cantilevered off the 3/4" aluminum. For a 60 kg inner conductor mass, the estimated deflection at the upstream end of the conductor is 5 mm.

The main water switch consists of a six electrode arrangement to minimize switch inductance. An electrode spacing of 4.8 cm should give a switchout voltage of 1.77 MV with a t_{eff} of 0.073 μs . The 3/4" thick aluminum plate the PFL conductors mount to also serves as a grounded prepulse shield to minimize capacitive coupling across the switch. After the load impedance has collapsed, a large fraction of the Marx energy is still left in the waterline, resulting in late time water breakdown. Therefore, stainless steel annuluses are inserted in the aluminum plate to serve as late time crowbar switches. The I.D. of these annuluses are easily changed to control the time of switching.

The output line is a 1.4 Ω coaxial line, supported by Delrin rods at 3 locations. A radial step is introduced to transition from the triaxial geometry of the PFL to a coaxial geometry. This transition leaves the line mechanically weak when subjected to shocks from the water switches, so tapered struts are utilized to stiffen the line. At the downstream end of the line are eight prepulse switches. An inductive transit time isolator is placed inside the line, which allows for signal and power lines to be routed to the diode anode. This isolator consists of a single turn 2" diameter aluminum tube supported at either end.

The downstream portions of the PFL conductors, the output line, and the vacuum insulator outer conductor are all fabricated using perforated stainless steel stock. This was done to allow for shock wave pressure relief when the water switches fire and to decrease the weight of the conductors. A FEMTO simulation was performed on a parallel plate geometry with one of the conductors having an 1/2" diameter hole "punched" out. The punched side of the material had a 0.08" radius around the hole and a 0.010" material deflection caused by the punching action. The electric field was then calculated as a function of the ratio of the enhanced area to the total area. This function was then integrated over the entire area and divided by the average electric field to obtain a perforation enhancement factor. For 1/16" thick material with 1/2" diameter holes staggered on 11/16" centers (48% open), the perforation enhancement factor was calculated to be 1.19. Table I summarizes the electric field values and breakdown fractions at key locations in the water section.

Table I— Select Breakdown Fractions

Region	Peak Voltage (kV)	t_{eff} (μs)	Area (cm^2)	Breakdown Strength (F) (kV/cm)	Max. E (E_m) (kV/cm)	E_m/F^1 (%)	E_m/F^2 (%)
ISC Intermediate Cond.	2500	0.5	1.5×10^5	146	110	75	
upstream end			4.6×10^3		120	82	
downstream end			2.3×10^3		130	89	
ISC Inner Cond.	2500	0.5	5.8×10^4	327	148	45	
downstream end			1.6×10^3		260	79	
PFL Intermediate Cond.	2600	0.18	1×10^5	209	155	74	88
downstream end	2400		5×10^3		210	100	
PFL Inner Cond.	2400	0.18	2.5×10^4	488	233	48	57
upstream end			700		400	82	
Output Line Inner Cond.	2400	0.064	1.3×10^4	331	216	65	77
downstream at interface	2000		4×10^3		264	80	

¹ w/ solid conductors

² w/ perforated conductors

The vacuum interface is shown in Figure 3. The surface flashover strength is calculated to be 112 kV/cm using the relation

$$F = 175t^{-0.167} A^{-0.1} \text{ kV/cm,}$$

with $t=0.062 \mu\text{s}$ and $A=9.4 \times 10^3 \text{ cm}^2$. To allow for delays in diode turn on which would result in a voltage as high as 2.4 MV across the interface, the interface is designed to operate at $\leq 80\%$ of flashover for the "baseline" voltage of 1.9 MV. Figure 3 shows the results of a FEMTO run on the vacuum insulator stack, with a maximum electric field of 93 kV/cm along the insulators' surface.

A new approach is being tried to divert a portion of the main pulse energy to drive the EMFAPS. Previously, on the LION accelerator, a plasma opening switch was used to transfer a small fraction of the main pulse to drive the anode

plasma source. This method had problems with reliability and reproducibility, so a method which capacitively couples a portion of the pulse energy in water is being employed. LION data indicates that a 10 ns, ≥ 50 kA current pulse which arrives 5-10 ns before the main pulse is required to evaporate the metal foil and establish the proper plasma parameters. An electrode is placed on the water side of the vacuum insulator inner conductor in close proximity to a grounded switch plate. The electrode spacing, as well as the radial position, can be adjusted with a minimal amount of effort. The signal generated is diverted to the anode foil using a 4 Ω transmission line through the inner conductor of the vacuum line.

CIRCUIT SIMULATIONS

EQUIPOTENTIAL PLOT

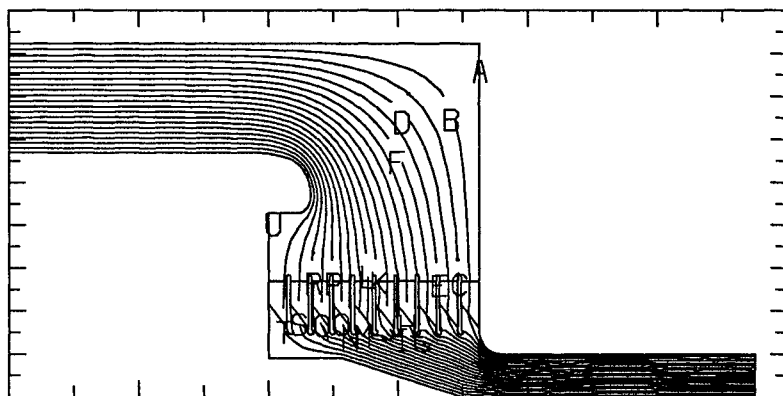


Figure 3 — Vacuum Insulator w/ Equipotential Lines (110 kV each)

Pspice² circuit analysis was used to model the FIREX pulser. Figure 4 shows schematically the circuit modeled. The Marx generator is modeled as a series RLC circuit with R selected to approximate the losses in the gas switches and capacitors. A value of 1 Ω is used (83 m Ω per stage), which is comparable with the 67 m Ω /stage calculated by Physics International for the PBFA II alternate Marx³ and the 75m Ω /stage recently measured on the new COBRA accelerator at Cornell University⁴. The circuit inductance modeled is 6 μ H, with 350 nH/stage and 1.8 μ H for Marx to ISC connections.

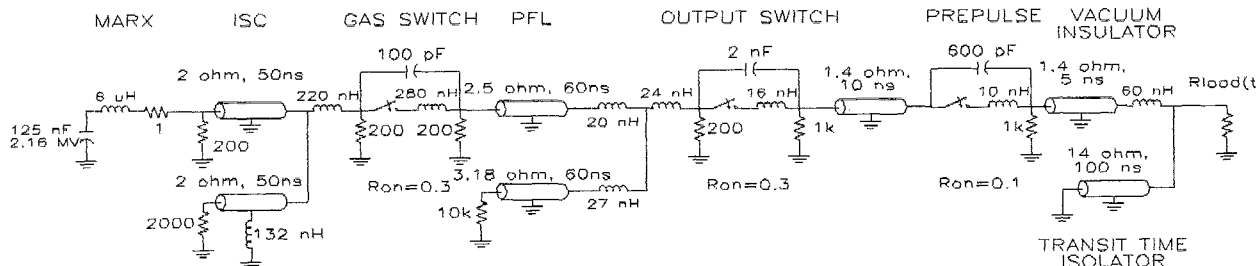


Figure 4 — Pspice Circuit Schematic used to Model FIREX Pulsed Power Generator

The triaxial ISC was modeled as two lossy transmission lines charged in series and discharged in parallel. The inner conductor support tubes account for the 132 nH inductance in the second line. The PFL also consists of two transmission lines charged in series and discharged in parallel. Gas and water switches were both modeled using the Pspice switch model is series with an inductor and in shunt with a capacitor. The main gas switch was modeled at $R_{off}=10$ k Ω and $R_{on}=0.3$ Ω , with an energy dissipation of 14 kJ. The water main and prepulse water switches were modeled with $R_{on}=0.3$ and 0.1 Ω , respectively, with $R_{off}=1$ k Ω . The dissipated energies were 27 and 18 kJ, respectively.

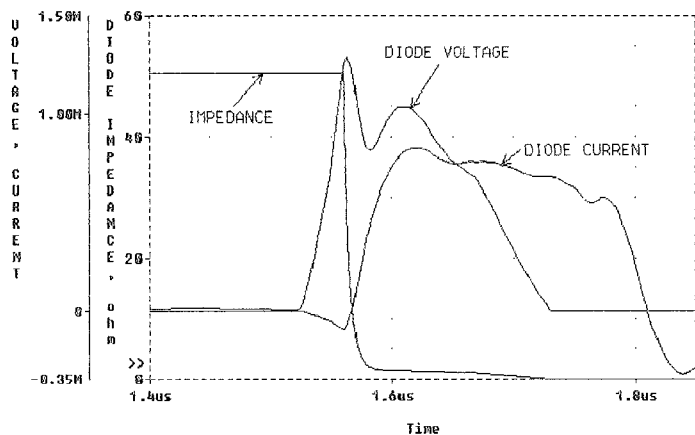


Figure 5 — Simulated Diode Signals

Figure 5 shows the final diode voltage, current, and impedance history from the Pspice simulation. The diode impedance history is based on data from the LION accelerator. Due to the shorter pulsewidth of the LION machine (40 ns), the diode impedance history was extrapolated for the longer pulsewidth seen in FIREX. A piece-wise linear variation after the exponential diode turn-on is used to model the impedance collapse. Baseline results indicate a peak diode voltage of 1.3 MV and a peak diode current of 830 kA. The pulsewidth, defined as the period where both current and voltage exceed 6×10^5 , is 86 ns, with 77 mC transferred to the diode when the voltage is greater than 600 kV.

A sensitivity analysis was performed to determine the variation of key operating parameters with changes in the circuit modeling. Table II shows the results of the analysis.

Table II — Circuit Model Parameter Sensitivity

Parameter Changed	Peak Diode Voltage (MV)	Peak Diode Current (kA)	Pulsewidth ¹ (ns)	Charge Transfer ² (mC)
Baseline	1.27	831	86	77.1
$C_{ISC}=45\text{nF}$ (50 baseline)	1.26	824	84	74.8
65 ns PFL (60 baseline)	1.13	795	86	77.8
55 ns PFL	1.38	841	84	76.0
$L_{VI}^3=70\text{ nH}$ (60 baseline)	1.20	813	84	76.5
$L_{VI}=90\text{ nH}$	1.10	785	80	73.6
Diode turn-on 10 ns early	0.83	834	85	77.7
Diode turn-on 10 ns late	1.68	818	85	75.3
$Z_{diode}=Z_{baseline}+0.4$	1.27	762	93	77.4
$Z_{diode}=Z_{baseline}-0.2$	1.27	870	76	72.6
$Z_{diode}=0$ 20 ns after baseline	1.27	823	97	84.0
$Z_{diode}=0$ 20 ns before baseline	1.27	841	70	66.9

¹time when V & I $\geq 600\text{k}$

²during period when V $\geq 600\text{ kV}$

³vacuum interface

ACKNOWLEDGMENTS

The authors would like to recognize the efforts of Juan Ramirez, David Smith, John Boyes, and other Sandia National Laboratories staff, in reviewing the electrical and mechanical design of the FIREX accelerator. Their comments and suggestions proved invaluable, and we are greatly appreciative. This work is supported by the Department of Energy under contract #DE-FG02-93ER54221.

REFERENCES

- 1Oppenheim, M.M., FEMTO User's Guide, V2.0, 1987.
- 2Pspice Version 5.0, MicroSim Corporation
- 3PBFA-II Energy Storage Section, Final Design Review Package, SNLA 26-4588, May 1983.
- 4private conversation w/ D.L. Smith, June 1995.